

PACS numbers: 42.55.Lt; 42.60.Da; 42.60.Jf
DOI: 10.1070/QE2007v037n01ABEH013295

Waveguide submillimetre laser with a uniform output beam

A.V. Volodenko, O.V. Gurin, A.V. Dyagterev, V.A. Maslov, V.A. Svich, A.N. Topkov

***Abstract*. A method for producing non-Gaussian light beams with a uniform intensity profile is described. The method is based on the use of a combined waveguide quasi-optical resonator containing a generalised confocal resonator with an inhomogeneous mirror with absorbing inhomogeneities discretely located on its surface and a hollow dielectric waveguide whose size satisfies the conditions of self-imaging of a uniform field in it. The existence of quasi-homogeneous beams at the output of an optically pumped 0.1188-mm waveguide CH_3OH laser with a amplitude-stepped mirror is confirmed theoretically and experimentally.**

Keywords: *CH_3OH laser, waveguide resonator, beam formation, single-mode regime.*

1. Introduction

Waveguide gas lasers find wide applications in various fields of science and technology [1]. A number of scientific and applied problems exist where the use of Gaussian laser beams formed in resonators with usual plane or spherical mirrors is not optimal. In laser applications in technologies for material surface machining, annealing of defects in semiconductors, lithography, location, in systems for optoelectronic data processing and medicine, it is desirable to use uniform output beams, i.e. beams with the uniform cross-sectional intensity distribution, which sharply decreases at the aperture edges. For practical applications, super-multimode [2], flattened Gaussian [3], and super-Gaussian radiation intensity profiles [4] have been proposed.

A specified intensity profile of the output beam in laser systems is obtained by using both external-cavity and intracavity methods [5]. In waveguide gas lasers, combined quasi-optical resonators are used, which contain multimode oversized waveguides and free-space regions. Therefore, methods for formation of the output beams of specified profile in such lasers should be based on a careful choice of geometrical parameters and matching of hollow waveguides and free-space regions to perform the coherent summation of transverse modes of the waveguide type [6].

In [7], a compact submillimetre laser with a waveguide resonator folded with the help of a set of fold mirrors is described. A set of fold mirrors is similar to the scheme of an open generalised confocal resonator [8], which increased its selectivity with respect to the fundamental mode and provided the uniform output beam of solid-state and gas IR lasers [9 – 11]. It was shown in [12, 13] that wave fields can be transmitted in multimode waveguides of certain size (polyharmonic waveguides) without distortions.

By using these approaches to the construction of laser resonators, we can realise a new method for obtaining the uniform output intensity profile in a waveguide laser based on a combined resonator containing a generalised confocal resonator with an inhomogeneous mirror and a polyharmonic waveguide. The aim of this paper is to built the experimental sample of a single-mode waveguide submillimetre laser with the uniform output beam based on such a resonator.

2. Theoretical relations

The theoretical consideration is based on the methods of eigenmodes and Fourier optics [14, 15]. The formation of resonator modes is described by the interference of the counterpropagating wave beams in the waveguide and free-space regions reflected by mirrors. The presence of phase correctors and inhomogeneities on mirrors will be described by using amplitude – phase correction functions [16]. We will substantiate the proposed principle of formation of a mode with the uniform intensity distribution on the output mirror (Fourier mode) by the example of a resonator with azimuthally symmetric circular reflectors.

Figure 1 presents the scheme of the resonator under study. The resonator contains circular dielectric waveguides (*1*) and (*1′*) of radius a_1 and length L_1 closed at one end by plane reflectors (*2*) and (*3*) with central coupling holes of radii a_4 and a_5, respectively, and optically coupled by fold mirrors through another end. The dimensions of waveguides should correspond to the self-imaging conditions for super-Gaussian radiation beams in hollow dielectric waveguides. These conditions were obtained in [17]. A set of fold mirrors consists of plane inhomogeneous mirror (*4*) of radius a_2 with an amplitude spatial filter located at the distance L_2 from two spherical mirrors (*5*) of radius a_3 located at the distance L_1 from waveguide ends. It is assumed that the transverse dimensions of the resonator elements satisfy the quasi-optical approximation $ka_i \gg 1$ (where $i = 1 - 5$, $k =$

A.V. Volodenko, O.V. Gurin, A.V. Dyagterev, V.A. Maslov, V.A. Svich, A.N. Topkov Department of Radiophysics, V.N. Karazin Kharkov National University, pl. Svobody 4, 61077 Kharkov, Ukraine; e-mail: Vyacheslav.A.Maslov@univer.kharkov.ua

Received 6 June 2006; revision received 13 July 2006
Kvantovaya Elektronika **37** (1) 63 – 68 (2007)
Translated by M.N. Sapozhnikov

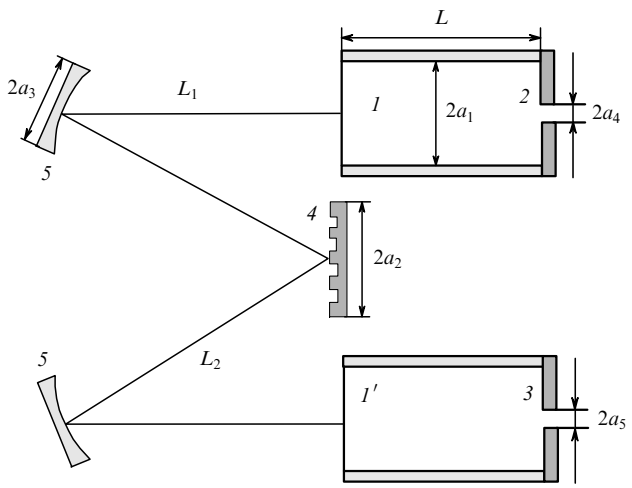

Figure 1. Scheme of a waveguide quasi-optical resonator with a amplitude-stepped mirror: (*1*, *1′*) hollow dielectric waveguides; (*2*, *3*) plane reflectors with coupling holes; (*4*) mirror with an amplitude spatial filter; (*5*) quadratic phase correctors.

$2\pi/\lambda$, λ is the wavelength) and the paraxial condition $k_{\|} \gg k_{\perp}$ (the longitudinal wave number is much greater than the transverse wave number). We assume that spherical mirrors are axially symmetric quadratic phase correctors with the focal distance F.

By using the method described in [18, 19], we reduce the problem of resonator eigenmodes to the system of integral equations

$$\alpha C_g = \exp(\mathrm{i}\gamma_g L) \sum_m \sum_n \sum_l \sum_p C_m B_{mn} D_{lp} b_{nl} b_{gp}$$

$$\times \exp[\mathrm{i}L(\gamma_n + \gamma_l + \gamma_p)], \quad g, l, m, n, p = 1, ..., M. \qquad (1)$$

Here, C_g is the coefficients of expansion of the required distributions of the complex amplitudes of oscillations of different types over M modes of the waveguide laser tube on the surface, for example, of plane reflector (*2*); α are the required eigenvalues of the system of equations (1) determining the energy losses $\delta_r = 1 - |\alpha|^2$ in the modes per round trip in the resonator and their phase shift $\arg\alpha$ additional to the geometrooptical shift; γ_i are the propagation constants of the waveguide modes [20];

$$B_{mn} = \int_0^1 U_m(\rho_1) U_n(\rho_1) F_2(\rho_1) \rho_1 \mathrm{d}\rho_1;$$

$$D_{lp} = \int_0^1 U_l(\rho'_1) U_p(\rho'_1) F_3(\rho'_1) \rho'_1 \mathrm{d}\rho'_1;$$

U_i are the orthonormalised distributions of the complex amplitudes of the waveguide modes of the laser tube [18]; $\rho_1 = r_1/a_1$ is the dimensionless radial coordinate for waveguide (*1*); ρ'_1 is the dimensionless radial coordinate for waveguide (*1′*);

$$F_2(\rho_1) = \begin{cases} 1, & d_4 \leqslant \rho_1 \leqslant 1, \\ 0, & 0 \leqslant \rho_1 < d_4, \end{cases} \quad F_3(\rho'_1) = \begin{cases} 1, & d_5 \leqslant \rho'_1 \leqslant 1, \\ 0, & 0 \leqslant \rho'_1 < d_5 \end{cases}$$

are the functions of the amplitude–phase correction of plane mirrors (*2*) and (*3*); $d_4 = a_4/a_1$; $d_5 = a_5/a_1$;

$$b_{ij} = \int_0^1 U_i(\rho_1) Q_j(\rho_1) \rho_1 \mathrm{d}\rho_1;$$

$$Q_j(\rho_1) = \int_0^1 Q^{(0)}(\rho_1, \rho'_1) U_j(\rho'_1) \rho'_1 \mathrm{d}\rho'_1;$$

$$Q^{(0)}(\rho_1, \rho'_1) = \frac{N_1 N_2}{(1 - G_1)(1 - G_2)}$$

$$\times \int_0^1 Q(\rho_1, \rho_2) Q(\rho_2, \rho'_1) T(\rho_2) \rho_2 \mathrm{d}\rho_2;$$

$$Q(\rho_1, \rho_2) = -4\pi^2 N_0 \exp[\mathrm{i}k(L_1 + L_2)] \exp[\mathrm{i}\pi(N_1\rho_1^2 + N_2\rho_2^2)]$$

$$\times \int_0^1 \exp[\mathrm{i}\pi(N_0 Z \rho_3^2) J_0(2\pi N_1 \xi_1 \rho_1 \rho_3) J_0(2\pi N_2 \xi_2 \rho_2 \rho_3) \rho_3 \mathrm{d}\rho_3;$$

$$Q(\rho_2, \rho'_1) = -4\pi^2 N_0 \exp[\mathrm{i}k(L_1 + L_2)] \exp[\mathrm{i}\pi(N_2\rho_2^2 + N_1\rho'^2_1)]$$

$$\times \int_0^1 \exp(\mathrm{i}\pi N_0 Z \rho_3^2) J_0(2\pi N_1 \xi_1 \rho_2 \rho_3) J_0(2\pi N_2 \xi_2 \rho'_1 \rho_3) \rho_3 \mathrm{d}\rho_3;$$

J_0 is the zero-order Bessel function of the first kind; $T(\rho_2)$ is the amplitude correction function for the inhomogeneous mirror; $\rho_2 = r_2/a_2$ and $\rho_3 = r_3/a_3$ are the dimensionless radial coordinates of the inhomogeneous mirror and phase correctors, respectively;

$$N_{1,2} = \frac{a_{1,2}^2}{\lambda L_{1,2}}; \quad N_0 = \frac{a_3^2}{\lambda F}; \quad \xi_{1,2} = \frac{a_3}{a_{1,2}};$$

$$G_{1,2} = 1 - \frac{L_{1,2}}{F}; \quad Z = \frac{1 - G_1 G_2}{(1 - G_1)(1 - G_2)}.$$

Let the distribution of the complex field amplitude on output mirror (*2*) of the waveguide quasi-optical resonator and, hence, on the end of the polyharmonic waveguide facing the phase corrector be described by the circular function

$$\mathrm{circ}\,\rho_1 = \begin{cases} 1, & \rho_1 \leqslant 1, \\ 0, & \rho_1 > 1. \end{cases} \qquad (2)$$

The Fourier–Bessel transformation of this function in the case of an infinitely long phase corrector has the form [15]

$$\mathrm{somb}\,\Theta = \frac{2J_1(\pi\theta)}{\pi\Theta}, \qquad (3)$$

with an accuracy to an insignificant constant factor, where $\Theta = 2N_{12}\rho_2$ and $N_{12} = a_1 a_2/[\lambda F(1 - G_1 G_2)]$ is the Fresnel number for the generalised confocal resonator.

By arranging absorbing elements on inhomogeneous mirror (*4*) so that $\rho_{2\chi} = v_{1\chi}/(2\pi N_{12})$ [where $v_{1\chi}$ are the roots of the equation $J_1(v_{1\chi}) = 0$, $\chi = 1, 2, 3, ...$], and taking into account the possibility of selecting transverse modes with the help of these elements [21], we can expect that

functions close to analytic forms (2) and (3) will be the solution of system (1). In this case, the transverse size of uniform regions at which boundaries the material constants experience a jump should considerably exceed the wavelength.

The system of equations (1) can be solved only by using a computer. The system was solved by the matrix method [22] with the help of the modified Rutishauser algorithm. There exist three independent forms of the solutions of system (1): for hybrid (EH_{nm}), transverse electric (TE_{0m}), and magnetic (TM_{0m}) modes, where n and m are the azimuthal and radial mode indices, respectively. The results of calculations presented below are related to practically important modes belonging to the class of axially symmetric EH_{1m} modes, which for $m \leqslant (a_1/\lambda)^{1/2}$ [23] have the liner polarisation of the field and complex amplitudes described by the complete system of orthonormalised functions $U_m(\rho_1) = \sqrt{2}J_0(Y_m\rho_1)/J_1(Y_m)$ [18], where J_0, J_1 are the Bessel functions of the first kind and Y_m are the roots of the equation $J_0(Y_m) = 0$. The propagation constants of these modes have the form [20]

$$\gamma_m \approx k\left[1 - \frac{1}{2}\left(\frac{Y_m\lambda}{2\pi a_1}\right)^2\left(1 - \frac{\mathrm{i}v_1\lambda}{\pi a_1}\right)\right],$$

where $v_1 = 0.5(v^2+1)/(v^2-1)^{1/2}$ and v is the refractive index of the waveguide wall.

3. Experimental setup

The scheme of the optically pumped submillimetre laser and experimental setup for its study is presented in Fig. 2. The submillimetre laser was pumped by a dc-discharge CO_2 laser. The linewidth of the CO_2 laser could be tuned within the P and R branches by using an echelette. The laser design is described in detail in [24]. A specific feature of the laser is that the echelette is located directly inside the discharge cavity, which allows removing an additional element (Brewster window) from the laser resonator, thereby increasing the output power and stability of the laser. The laser operates in the regime of slowly circulating $CO_2 : N_2 : He : Xe = 1 : 1 : 4 : 0.25$ working mixture. By rotating echelette (*6*), the laser can be tuned to any of 80 lines of the P and R branches in the wavelength range from 9.2 to 10.6 μm. Resonator mirror (*3*) was mounted on piezoelectric corrector (*4*) to provide continuous frequency tuning within the gain line with the help of direct-current source (*5*). The output power of the laser was no less than 15 W at any of the lines of the P and R branches. The CO_2 laser radiation was focused by plane mirror (*11*) and spherical mirror (*12*) (with the radius of curvature of 500 mm) on the coupling hole of the resonator of the submillimetre cell.

The submillimetre cell represents a vacuum chamber made of a glass tube with the internal diameter 80 mm and length 610 mm. The resonator is formed by two quartz waveguides (*15*) of diameter 9.6 mm and length 470 mm. The waveguide length $L \approx 2.4\,a_1^2/\lambda$ was chosen to correspond to the self-imaging conditions for super-Gaussian radiation beams in hollow dielectric waveguides [17]. Phase correctors playing the role of the elements of a Fourier transformer in the calculation model of the laser resonator are two spherical mirrors (*17*) of diameter 40 mm with the focal distance 80 mm. To remove the frequency degeneracy

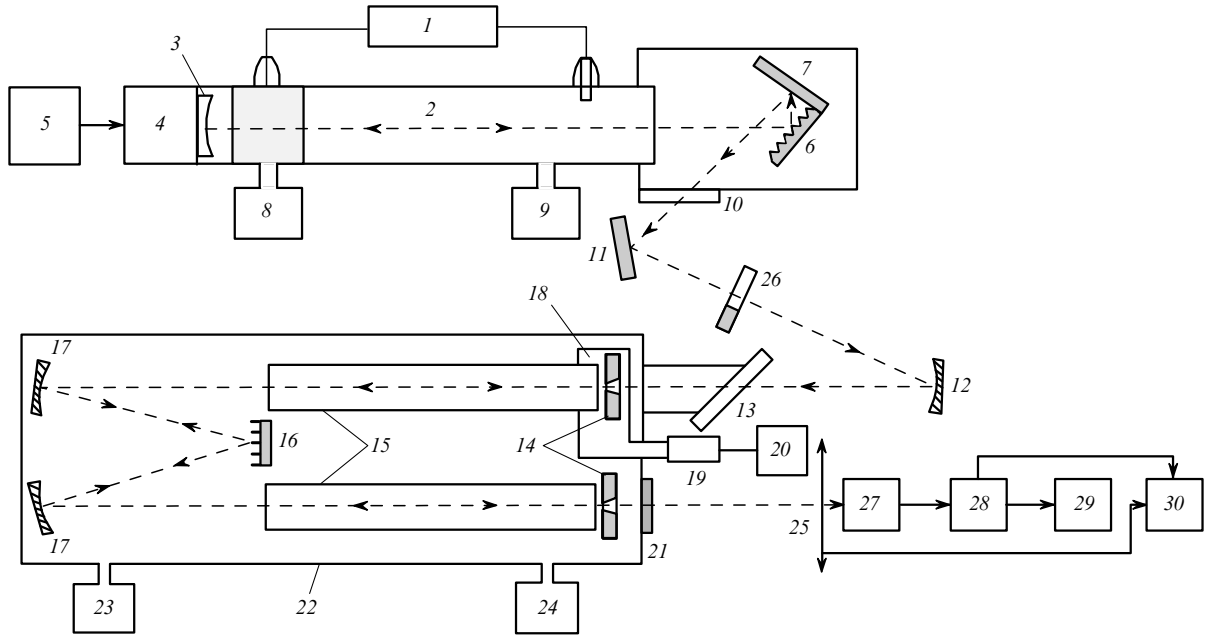

Figure 2. Scheme of the submillimetre laser with a amplitude-stepped mirror: (*1*) high-voltage power supply of a CO_2 laser; (*2*) discharge tube; (*3*) spherical mirror; (*4*) piezoelectric element; (*5*) dc voltage source; (*6*) diffraction grating; (*7*) corner reflector; (*8*) CO_2 laser evacuation system; (*9*) system for CO_2 laser working mixture filling; (*10*), (*13*) NaCl plates; (*11*) plane mirror; (*12*) spherical mirror; (*14*) mirrors with coupling holes; (*15*) quarts waveguides; (*16*) amplitude-stepped mirror; (*17*) spherical fold mirrors; (*18*) resonator mirror displacement device; (*19*) micrometric screw; (*20*) electric motor; (*21*) quartz plate; (*22*) vacuum volume; (*23*) submillimetre cell evacuation system; (*24*) system for filling the submillimetre cell with the working gas; (*25*) azimuthal detector displacement device; (*26*) mechanical modulator; (*27*) submillimetre radiation detector; (*28*) amplifier; (*29*) oscilloscope; (*30*) chart recorder.

of resonator modes [25], the phase correctors are located at distances from the waveguide ends and mirror (*16*) that are approximately equal to their focal distances ($G_1 = G_2 = -0.01$). As mirror (*16*), we used in experiments a plane glass mirror of diameter 12 mm with an aluminium coating and an aluminium inhomogeneous amplitude-stepped mirror of the same diameter. It is also employed as one of the fold mirrors. The parameters of the inhomogeneous mirror were preliminarily calculated from (1), and after its fabrication, the measured widths of reflecting rings and absorbing grooves were again substituted into (1) and the mode parameters were calculated for the real model of the resonator.

The inhomogeneous mirror in the form of alternating reflecting rings and absorbing grooves was fabricated by the mechanical method by using a special cutter. Absorbing grooves were stitched by a cutter to a depth of $\sim$0.2 mm (1.68λ) at an angle of 30° to the reflecting plane of the mirror. As a result, beams reflected from the surface of grooves were coupling out of the laser resonator, which is similar to almost complete absorption of radiation in these grooves. The diameter of the central reflecting part of the mirror was measured to be 2.52 ± 0.01 mm ($21.21\lambda \pm 0.08\lambda$). The widths of reflecting rings and adjacent absorbing grooves are presented in Table 1.

Table 1.

N	Ring width		Groove width	
	in units of λ	mm	in units of λ	mm
1	10.60	1.26	3.03	0.36
2	6.57	0.78	3.03	0.36

Note: N is the ordinal number of the arrangement of grooves and rings with respect to the mirror centre.

Resonator mirrors (*14*) are plane copper mirrors with central coupling holes of diameter 2 mm. Our calculations showed that for coupling holes of such a diameter, the field on mirrors (*14*) virtually coincides with the field on mirrors without holes. All the resonator elements are mounted on a common bench, where device (*18*) of plane–parallel displacement is also placed on which one of mirrors (*14*) is mounted. The mirror is displaced by micrometric screw (*19*) located outside the vacuum volume. The mirror can be displaced automatically with the help of electric motor (*20*).

Evacuating and gas-filling systems (*23*) and (*24*) provide the filling of the submillimetre cell with the working mixture and maintain the optimal pressure for obtaining the maximum output power. Laser radiation is detected by pyroelectric detector (*27*) with U2-8 amplifier (*28*) and is recorded with C1-93 oscilloscope (*29*) and KSP 4 chart recorder (*30*). The detector is fixed in the device of azimuthal displacement. The chart recorder was synchronised with devices of detector or resonator mirror displacement. The diameter of the photosensitive area of the detector was 2 mm. The emission spectrum of the laser was studied by placing on the detector a conic head with the input diameter of 20 mm.

4. Comparison of experimental and numerical results

The wavelength of submillimetre radiation was 0.1188 mm. The parameters of the active medium in calculations were set equal to those of an optically pumped waveguide CH_3OH laser with a slowly circulating working mixture. The small-signal gain was $g_0 = 0.64$ m^{-1} and the saturation intensity for the emission transition was $I_s = 0.0725$ kW cm^{-2} [26]. The waveguide walls were made of silica glass with the refractive index $v \approx 2.32 + i \times 0.40$ at $\lambda = 0.1188$ mm [27].

The output power P of the laser was calculated by the method described in [28, 29] by using the Rigrod expression [30]

$$P = \frac{\delta_{out}}{\delta_t} I_s V \left[g_0 - 0.5 \frac{1}{(1-\delta_t) L_d} \right], \quad (4)$$

where δ_{out} is coupling losses; V is the volume of the generated resonator mode; L_d is the amplifying discharge length; $\delta_t = \delta_r + \delta_h$ are total mode losses per round trip in the resonator; and δ_h are thermal losses in reflectors. The mode volume V of the laser beam in the resonator was calculated from the expression

$$V = 2\pi^2 \int_0^L \int_0^1 \frac{I(\rho, z)}{I_{max}(\rho, z)} a_z^2 \rho d\rho dz, \quad (5)$$

where $\rho = r/a_z$ is the dimensionless radial coordinate for waveguide channels and free-space regions in the resonator; $I(\rho, z)$ and $I_{max}(\rho, z)$ are the current and maximal values of the field intensity in different cross sections of the resonator, respectively; and a_z is the radius of these cross sections. The total thermal losses in resonator reflectors are set equal to 10 %.

The output power P of the waveguide CH_3OH laser calculated from relations (4) and (5) by using homogeneous mirror (*16*) (Fig. 2) was 1.5 mW for the mode volume for the lowest resonator mode equal to $V = 60.1$ cm^3. When amplitude-stepped mirror (*16*) was used with parameters presented in section 2, which were optimal for obtaining a uniform field on the output mirror, the calculated output power of the waveguide CH_3OH laser was 1 mW for the mode volume of the Fourier mode equal to $V = 65.4$ cm^3. The output power of the laser measured with homogeneous and inhomogeneous mirror (*16*) was 0.7 and 0.5 mW, respectively. Measurements were performed by using a BIMO-1 bolometer. Some discrepancy between calculations and experiment can be explained by the difference of the parameters g_0 and I_s of the active medium used in calculations from real parameters, and the difference between the theoretical and experimental waveguide parameters (ellipticity, surface roughness, etc.), as well as by the neglect of the orientation of phase correctors (fold mirrors) at some angles to the waveguide axes.

Figure 3 presents the output tuning curves of the laser with homogeneous and amplitude-stepped mirror (*16*). One can see from Fig. 3a that, when the homogeneous mirror was used, the three lowest (in losses) resonator modes EH_{1m} were observed with changing the resonator length. According to our calculations, losses in these modes per pass are 27.67 %, 76.26 %, and 89.88 %, respectively. When the amplitude-stepped mirror was used in the laser, only one (Fourier) mode was observed in the tuning curve (Fig. 3b). Losses in this mode per pass were 34.18 %, while losses in the two next (in Q factor) modes were 80.72 % and 95.07 %, respectively. The use of an inhomogeneous mirror in the laser increases losses of the pump radiation [31], resulting in

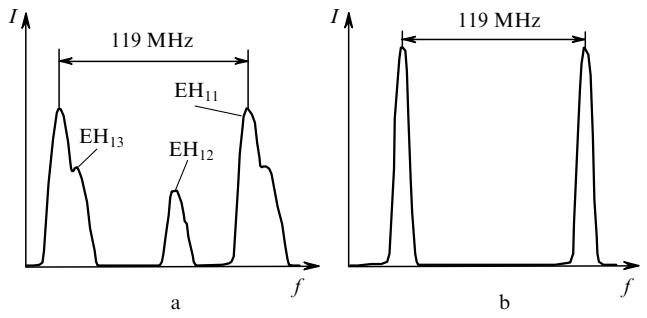

Figure 3. Tuning curves of the waveguide CH_3OH laser with the homogeneous (a) and amplitude-stepped (b) mirrors.

the decrease in the gain in the active medium and the absence of higher modes in the emission spectrum.

Table 2 presents the calculated frequency differences for the first and second (f_{12}), the first and third (f_{13}) modes for the laser with homogeneous and amplitude-stepped mirror (*16*) and experimental frequency differences for these modes generated with the homogeneous mirror. The discrepancy between the calculated and experimental data can be explained by the frequency pulling in the laser and by some difference between geometrical dimensions of the laser used in calculations and their real values.

Table 2.

Mirror type	Calculation		Experiment	
	f_{12}/MHz	f_{13}/MHz	f_{12}/MHz	f_{13}/MHz
Homogeneous	54.74	14.28	46.41	10.71
Step-amplitide	58.31	38.08		

Figure 4 shows the transverse intensity and phase distributions of the field on output mirror (*14*) calculated for homogeneous and amplitude-stepped mirror (*16*). The normalised absolute measure of discrepancy Π between the circular function $\mathrm{circ}\,\rho_1$ and the field intensity profile $I(\rho_1)$ on the output mirror with an inhomogeneous mirror in the resonator, defined as [32]

$$\Pi = \frac{1}{S}\sum_{s=1}^{S} |1 - I(\rho_{1s})|$$

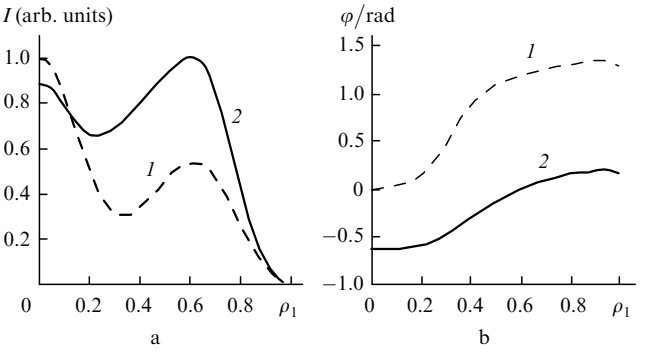

Figure 4. Radial intensity (a) and phase (b) distributions on the output mirror of the laser calculated for the homogeneous (*1*) and amplitude-stepped (*2*) reflectors.

(where S is the number of points of the discrete specification of the field), does not exceed 30 %.

To confirm the fact that the radial intensity profile obtained on output mirror (*14*) of the CH_3OH laser is close to the homogeneous function $\mathrm{circ}\,\rho_1$, we studied experimentally and numerically the far-field transverse laser radiation intensity distributions. Figure 5 presents the calculated and experimental far-field intensity distributions of laser radiation at distances 380 and 670 mm from output mirror (*14*) with a coupling hole of diameter 2 mm in the case of amplitude-stepped mirror (*16*). The calculated and experimental FWHMs of these distributions are coincident. The calculated and experimental intensity profiles observed at a distance of 670 mm are in good agreement. Some discrepancy between the transverse intensity distributions measured at a distance of 380 mm can be explained by small differences between the theoretical and experimental parameters of the active medium, shape (ellipticity), and size of the coupling hole.

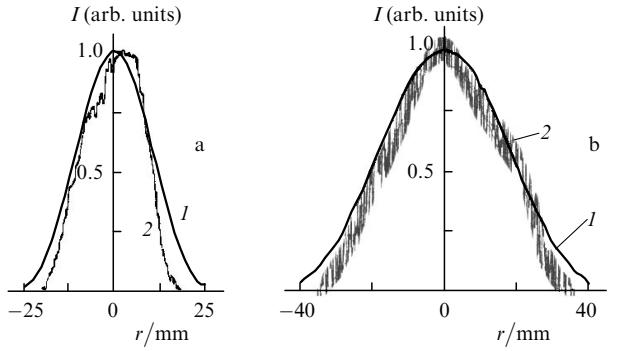

Figure 5. Calculated (*1*) and experimental (*2*) radial distributions of the radiation field intensity for the laser with the amplitude-stepped mirror at distances of 380 (a) and 670 mm (b) from the output mirror.

Thus, we proposed and studied experimentally the optically pumped submillimetre laser with the uniform output beam profile. The laser is based on a combined waveguide quasi-optical folded resonator including a generalised confocal resonator with an inhomogeneous amplitude-stepped mirror and a polyharmonic waveguide. It has been shown that the method of intracavity formation of uniform output beams in waveguide lasers can also provide the suppression of higher modes in such lasers.

Acknowledgements. The authors thank A.Ya. Anikeev for his help in the fabrication of the amplitude-stepped mirror.

References

1. Ochkin V.N. *Volnovodnye gazovye lazery* (Waveguide Gas Lasers) (Moscow: Znanie, 1988).
2. Borghi R., Santarsiero M. *IEEE J. Quantum Electron.*, **35**, 745 (1999).
3. Gory F. *Opt. Commun.*, **107**, 335 (1994).
4. Santarsiero M., Borghi R. *J. Opt. Soc. Am. A*, **16**, 188 (1999).
5. Oron R., Davidson N., Hasman E., Friesem A.A., in *Progr. in Optics* (Amsterdam: Elsevier, 2001) Vol. 42, p. 325.
6. Bokut' B.V., Romanenko E.S., Khilo N.A. *Kvantovaya Elektron.*, **18**, 985 (1991) [*Sov. J. Quantum Electron.*, **21**, 893 (1991)].
7. Gurin O.V., Dyagterev A.V., Maslov V.A., et al. *Kvantovaya Elektron.*, **31**, 346 (2001) [*Quantum Electron.*, **31**, 346 (2001)].

8. Vakhitov N.G., Isaev M.P., Kushnir V.R., Sharif G.A. *Kvantovaya Elektron*., **14**, 1633 (1987) [*Sov. J. Quantum Electron*., **17**, 1037 (1987)].
9. Büttner A., Kowarschik R., Zeitner U.D. *Appl. Phys. B*, **81**, 601 (2005).
10. Gurin O.V., Epishin V.A., Maslov V.A., et al. K*vantovaya Elektron*., **25**, 424 (1998) [*Quantum Electron*., **28**, 411 (1998)].
11. Gurin O.V., Epishin V.A., Maslov V.A., et al. *Kvantovaya Elektron*., **31**, 543 (2001) [*Quantum Electron*., **31**, 543 (2001)].
12. Rivlin L.A., Shil'dyaev V.S. *Izv. Vyssh. Uchebn. Zaved., Ser. Radiofiz*., **11**, 572 (1968).
13. Grigor'eva E.E., Semenov A.T. *Kvantovaya Elektron*., **5**, 1877 (1978) [*Sov. J. Quantum Electron*., **8**, 1063 (1978)].
14. Kazenelenbaum B.Z. *Vysokochastotnaya elektrodinamika* (High-Frequency Electrodynamics) (Moscow: Nauka, 1966).
15. Goodman J.W. *Introduction to Fourier Optics* (New York: McGraw-Hill, 1968; Moscow: Mir, 1970).
16. Epishin V.A. *Kvantovaya Elektron*., **5**, 1263 (1978) [*Sov. J. Quantum Electron*., **8**, 720 (1978)].
17. Gurin O.V., Maslov V.A., Svich V.A., et al., in *Radiotekhnika* (Radio Engineering) (Kharkov: Kharkov National University of Radioelectronics, 2001) No. 121, p. 117.
18. Abrams R.L., Cherster A.N. *Appl. Opt*., **13**, 2117 (1974).
19. Gurin O.V., Maslov V.A., Svich V.A., et al., in *Radiotekhnika* (Radio Engineering) (Kharkov: Kharkov National University of Radioelectronics, 2001) No. 127, p. 104.
20. Marcatili E.A.J., Schmeltzer R.A. *Bell. Syst. Techn. J*., **43**, 1783 (1964).
21. Epishin V.A., Lytov A.V., Kamyshan V.A. *Trudy V Vsesoyuznogo simpoziuma po difraktsii i rasprostraneniyu voln* (Proceedings of V All-Union Symposium on Wave Diffraction and Propagation) (Leningrad: Nauka, 1971) p. 91.
22. Sanderson R.L., Streifer W. *Appl. Opt*., **8**, 131 (1969).
23. Epishin V.A., Maslov V.A., Ryabykh V.N., et al. *Radiotekh. Elektron*., **33**, 700 (1988).
24. Berezhnyi V.L., Kononenko V.I., Pavlichenko O.S., Shabanov Yu.E., Anikeev A.Ya., Didenko V.N., Epishin V.A., Pokormyakho N.G., Svich V.A., Topkov A.N., Tkachenko V.M. Preprint of Kharkov Institute of Physics and Technology, Akad. Nauk USSR, No. 87 – 37 (Kharkov, 1987).
25. Valitov R.A. (Ed.) *Tekhnika submillimetrovykh voln* (Techniques of Submillimetre Waves) (Moscow: Sov. Radio, 1969).
26. Dyubko S.F., Fesenko L.D. Preprint of Institute of Radiophysics and Electronics, Akad. Nauk USSR, No. 137 (Kharkov, 1979).
27. Birch J.R., Cook R.J., Harding A.F., et al. *J. Phys. D: Appl. Phys*., **8**, 1353 (1975).
28. Siegman A.E., Sziklas E.A. *Appl. Opt*., **13**, 2775 (1974).
29. Gurin O.V., Maslov V.A., Svich V.A., Topkov A.N. *Proc. II Int. Conf. on Advanced Optoelectronics & Lasers* (Alushta, Ukraine, 2003) Vol. 1, p. 140.
30. Tarasov L.V. *Fizika protsessov v generatorakh kogerentnogo opticheskogo izlucheniya* (Physics of Processes in Lasers) (Moscow: Radio i svyaz', 1981).
31. Gurin O.V., Dyagterev A.V., Maslov V.A., et al. *Vestn. Khar'kov National University*, No. 570 (2), 50 (2002).
32. Herman G.T. *Image Reconstruction from Projection: the Fundamentals of Computerized Tomography* (New York: Academic Press, 1980; Moscow: Mir, 1983).